

Monolayers of Diblock Copolymer at the Air-Water Interface: The Attractive Monomer-Surface Case

M. C. Fauré⁽¹⁾, P. Bassereau⁽¹⁾, M. A. Carignano⁽²⁾, I. Szleifer⁽³⁾, Y. Gallot⁽⁴⁾ and D. Andelman⁽⁵⁾

⁽¹⁾*Physico-chimie Curie, UMR 168 CNRS, Institut Curie*

11, rue Pierre et Marie Curie, 75231 Paris Cedex 05 France

⁽²⁾*Department of Chemical Engineering, University of Delaware, Newark, DE 19716, USA*

⁽³⁾*Department of Chemistry, Purdue University, West Lafayette, IN 47907-1393, USA*

⁽⁴⁾*Institut C. Sadron, 6, rue Boussingault, 67083 Strasbourg cedex, France*

⁽⁵⁾*School of Physics and Astronomy, Raymond and Beverly Sackler Faculty of Exact Sciences*

Tel Aviv University, Ramat Aviv 69978 Israel

(June 4, 1997)

We have studied both experimentally and theoretically the surface pressure isotherms of copolymers of polystyrene-polyethyleneoxide (PS-PEO) at the air-water interface. The SCMF (single chain mean-field) theory provides a very good agreement with the experiments for the entire range of surface densities and shows that the adsorption energy per PEO monomer at the air-water interface is about one $k_B T$. In addition, the chain density profile has been calculated for a variety of surface densities, from the dilute to the very dense ones. The SCMF approach has been complemented by a mean-field approach in the low density regime, where the PEO chains act as a two-dimensional layer. Both theoretical calculations agree with the experiments in this region.

I. INTRODUCTION

Insoluble monomolecular layers at interfaces have been the subject of many experimental and theoretical studies since the pioneering works of I. Langmuir [1–3]. These studies have been performed on small amphiphilic molecules such as surfactants and lipids at the gas-liquid or solid-liquid interface.

More recently, the structure of quasi two-dimensional layers of long polymer chains at interfaces have been investigated theoretically and experimentally. The polymer layers can be obtained in three different situations: (i) the polymer chains are grafted to the interface by one end. This scenario has inspired many theoretical studies [4–8] especially in the high surface density regime where elongated chain conformations called “*brushes*” are expected. Experimental studies [9–11] exist in the brush regime as well for the low and intermediate surface grafting densities.

(ii) In another scenario the polymer chains are adsorbed onto the interface from a liquid solution due to weak attractive interactions with the interface. Concentration profiles of the polymers as a function of the distance from the interface have been measured using neutron scattering and neutron reflectivity for polymers adsorbed from solution onto a solid substrate [12–15] and onto an air-liquid interface [16]. This scenario was also addressed theoretically [5,17–19].

(iii) A monolayer of a diblock copolymer is spread at the air-liquid interface provided that one block is soluble in the aqueous subphase while the other is hydrophobic and acts as the grafting end of the chain [20–25]. Similarly to the case of Langmuir monolayers of short chains, the grafting density of the diblock can be changed continuously by moving a barrier on the air-liquid interface, hence changing the surface pressure. Since the grafting density is a controlled parameter, different monolayer regimes can be tested in one experiment offering a big advantage over polymer systems grafted or adsorbed on solid surfaces.

In the present work we address only the latter situation of a diblock copolymer system at the air-liquid interface. Even here one can consider two different cases as was realized experimentally. In the first, the block soluble in the liquid subphase has no surface activity. Such a case has been studied, e.g., by Kent et al. [20]. In the second case, the block soluble in the liquid subphase is attracted to the air-liquid interface. This was realized experimentally by a diblock copolymer composed of a polyethylene oxide (PEO) and a polystyrene (PS) blocks. The PEO homopolymer is soluble in water and is known to adsorb spontaneously [21,22] on the air-water interface as can be easily inferred from the surface pressure isotherm showing a “pseudo-plateau” at medium surface pressures. Upon further increase in the surface pressure, the adsorbed PEO layer becomes unstable. It is not possible to obtain a very condensed surface layer since the monomers can detach from the surface and dissolve in the bulk aqueous solution. However, if the PEO chain is linked chemically to another, water insoluble, chain (like a PS block), further compression of the diblock copolymer into its brush-like regime can be achieved [23,24].

In a previous study of the PS-PEO copolymer [25], different PEO chain lengths and a PS block of 40 monomers have been used. A model based on a numerical version of the self-consistent field (SCF) theory was proposed [25] and

took into account the adsorption of the PEO monomers on the water surface. The model predicts in a qualitative way the experimental isotherms for the PS-PEO monolayer and, in particular, the existence of a pseudo-plateau on the isotherm. From neutron reflectivity data, the progressive stretching of the chains in the high surface density region is confirmed by fitting of the results to the expected parabolic-shape concentration profile [4].

Although our study is mainly motivated by fundamental issues related to pseudo two-dimensional polymer layer, it is of relevance to important biomedical applications where derivatives of PEO are used to modify adhesion properties of surfaces and interfaces. We mention two examples. In the first, grafting of polymers (in particular PEO with a hydrophobic group or block) to hydrophobic surfaces is a very promising way to avoid non-desired protein adsorption onto specific surfaces [26,27]. This type of surface modification has great potential in increasing the biocompatibility of various materials. The second application relates to grafting of PEO onto bilayers of liposomes. It has been shown that such a grafting increases the longevity of these liposomes in the blood stream, making them practical vehicles for enhanced drug delivery [28]. In the above two examples, the main function of the polymer layer is to form a steric barrier in order to prevent the adhesion of proteins and other cells in the blood stream.

In the present work we further investigate experimentally pressure isotherms of several PS-PEO systems in the condensed as well as in the dilute and intermediate surface density regimes. We use the single chain mean-field (SCMF) theory to calculate pressure isotherms and concentration profiles of the experimental PS-PEO copolymer system. The SCMF approach has been used successfully to predict the structural and thermodynamical properties of polymer systems [8,29,30]. The predicted and measured pressure isotherms are in very good agreement in the entire surface density range. The only adjustable parameter, the adsorption energy of the PEO monomers, is found to be roughly one $k_B T$. The SCMF calculation is complemented by a mean-field approach in the low surface density regime, assuming a two-dimensional layer of the PS-PEO copolymer. Up to the plateau, there is a very good agreement between the two theoretical approaches and also with the experimental data.

Our paper is organized as follow: in the Sec. II we will present our experimental technique. Section III describes the SCMF theory. The experimental results on surface pressure isotherms for PS-PEO copolymers with various PS and PEO block sizes and the predictions of the SCMF theory are presented in Sec. IV. The section ends with the mean-field calculation and predictions. Finally, Sec. V is devoted to a discussion of the different results.

II. MATERIALS AND EXPERIMENTAL TECHNIQUE

A. Materials

We have used asymmetric diblock copolymers synthesized by sequential anionic polymerization. The hydrophobic block consists of a polystyrene (PS) chain having between 13 and 43 monomers. Each monomer has a molecular weight of 104 g/mole. The hydrophilic block is a polyethylene oxide (PEO) chain that is OH terminated. The number of PEO monomers varies between 64 and 700, each having a molecular weight of 44 g/mole. In the following, the PS-PEO copolymer chains will be denoted as $N_{\text{PS}}-N_{\text{PEO}}$ where N_{PS} is the number of PS monomers and N_{PEO} the number of PEO monomers. The copolymers used in this work have a small polydispersity and their properties are listed in Table 1. We note that the 31- N_{PEO} copolymers have a partially deuterated PS block. However, this has no particular importance for the present study.

B. Surface Isotherms

The surface pressure isotherms have been obtained with a teflon Langmuir film balance (Lauda – FW 2) at $T = 18^\circ \text{C}$ in a clean room. The maximum available surface is 927 cm^2 and can be varied continuously by moving a Teflon barrier. The surface pressure Π is measured with a Langmuir balance. The Langmuir film is obtained by depositing a small drop (with a micro syringe) of about $100 \mu\text{l}$ of the copolymer in a chloroform solution on the air-water interface. The copolymer concentration is a few g/l.

Before compression, the film is allowed to equilibrate for about 15 minutes to ensure full evaporation of the solvent and also to allow a re-adjustment of the molecules. This re-adjustment is clearly more important for these long chains than for short-chain surfactant molecules. The compression rate is kept constant at $55 \text{ \AA}^2/\text{molecule}/\text{min}$. We have checked that the isotherms are unchanged when lower rates down to $2 \text{ \AA}^2/\text{molecule}/\text{min}$ are used. As the copolymer chain length used here varies by a factor ten, we adjusted accordingly the speed of the barrier displacement in order to ensure the same compression rate (per monomer) in all the samples.

III. MOLECULAR THEORY

In this section we briefly describe the molecular approach that we use in order to explain the experimental observations. The theoretical approach is the single-chain mean-field (SCMF) theory which was originally developed to treat packing of chains in surfactant aggregates [31] and later was generalized for tethered polymer layers [8]. This theory has been widely applied in a variety of polymer systems. The predicted structural and thermodynamic properties are in good agreement with experiments [20,30] and with full scale Monte Carlo and molecular dynamics computer simulations [7]. Here we present a short derivation of the theory concentrating on the points which are most relevant to the PS-PEO monolayer. For an extensive discussion of the derivation and application of the SCMF theory to tethered polymer layers, the reader is referred to a recent review article [8].

A. Formalism

The basic idea of the SCMF theory is to consider a central chain while taking into account exactly all its *intramolecular* and surface interactions, and treating the *intermolecular* interactions within a mean-field approximation. The configurations of the central chain are treated explicitly and the probability of the different conformations changes as a function of the intermolecular (mean-field) interactions. Those latter interactions depend upon the thermodynamic variables of the system, e.g., surface coverage and temperature. The probability distribution function (pdf) of chain conformations is determined by minimizing the system free-energy subject to the local incompressibility assumption. We note that the SCMF theory is different from the self-consistent field (SCF) which was used in a previous study [25] of the PS-PEO system. These differences are further discussed in Ref. [8]. The SCMF theory can be applied in the entire range of surface coverage, from the very dilute to concentrated coverages, and for different types of solvents: good, bad and in Θ conditions.

We model the PS-PEO layer at the air-water interface as two monolayers. One is composed of PS segments and resides on the air side of the interface. The other is the PEO layer residing on the water side. We assume that the interface is sharp on molecular length scales. While this is not a necessary condition it simplifies the calculations without affecting the results in any substantial way. It is, therefore, assumed that there is no coupling between the PS and the PEO monolayers other than the fact that they both have the same surface coverage. The theory presented below is applied for treating a tethered polymer layer, with specific parameters chosen in order to represent the experimental PS-PEO copolymer layers as shown in Sec. IV.

The central quantity of the theory is the probability distribution function (*pdf*) of chain conformations. From the knowledge of the *pdf* any desired conformational and thermodynamic averaged quantity can be determined. The total free energy (per unit area) of the polymer layer can be written in terms of different entropy and energetic contributions:

$$\frac{W}{A} = -T(S_{c,pol} + S_{t,pol} + S_{t,solv}) + \sigma \langle \epsilon_{intra} \rangle + \sigma \langle \epsilon_{inter} \rangle + \sigma \langle \epsilon_{s-p} \rangle \quad (1)$$

where T is the temperature. The six contributions to the free energy are listed below and all depend on averages with respect to the *pdf* of chain conformations, $P(\alpha)$.

- i.* The conformational entropy of the chain molecules $S_{c,pol} = -k_B \sigma \sum_{\{\alpha\}} P(\alpha) \ln P(\alpha)$, where k_B is the Boltzmann constant; $\sigma = \mathcal{N}/A = 1/\Sigma$ denotes the polymer surface density with \mathcal{N} and A being, respectively, the total number of molecules and the area of the interface, and Σ the area per chain. The sum runs over all possible chain conformations $\{\alpha\}$.
- ii.* The translational entropy of the polymer chains, $S_{t,pol} = -k_B \sigma \ln l^2 \sigma$, where l is the polymer segment length and l^2 is approximately the compact area per segment at the interface.
- iii.* The internal energy of the polymer-solvent mixture. One can show that this energy can be written in terms of polymer-polymer attractive interactions including both intra- and intermolecular contributions as well as the surface-polymer (interface) interactions.

The intramolecular contribution is $\langle \epsilon_{intra} \rangle = \sum_{\{\alpha\}} P(\alpha) \epsilon_{intra}(\alpha)$. The energy $\epsilon_{intra}(\alpha)$ includes the sum of all non-bonded pairs of segments, which are taken to interact attractively as the tail of a Lennard-Jones potential.

The surface-polymer interaction is $\langle \epsilon_{s-p} \rangle = \int_0^\delta \chi_{s-p} \langle n(z) \rangle dz$, where χ_{s-p} is the strength of the surface-polymer interaction. The average number of segments of the central chain at distance z from the interface is given by $\langle n(z) \rangle dz = \sum_{\{\alpha\}} P(\alpha) n(\alpha, z) dz$, where $n(\alpha, z) dz$ is the number of segments that a chain in conformation α

has at distance z from the surface. It is assumed that all monomers within a distance $0 \leq z \leq \delta$ from the surface interact with the surface. This contribution will turn out to be very important in understanding the experimental PS-PEO pressure-area isotherms.

The intermolecular contribution has the form

$$\langle \epsilon_{inter} \rangle = \frac{1}{2\sigma l^4} \int \int \chi(|z - z'|) \langle \phi_p(z) \rangle \langle \phi_p(z') \rangle dz dz' = \frac{\sigma l^2}{2} \int \int \chi(|z - z'|) \langle n(z) \rangle \langle n(z') \rangle dz dz' \quad (2)$$

where the factor $\frac{1}{2}$ corrects the double counting of the integral, $\chi(|z - z'|)$ is the distance dependent van der Waals interaction parameter (in units of $k_B T$), and $\langle \phi_p(z) \rangle = \sigma l^3 \langle n(z) \rangle$ is the average volume fraction of polymer in the layer defined between z and $z + dz$.

iv. The translational entropy of the solvent molecules,

$S_{t,solv} = -k_B l^{-3} \int \langle \phi_s(z) \rangle \ln \langle \phi_s(z) \rangle dz$, where $\langle \phi_s(z) \rangle$ is the average volume fraction of the solvent at distance z . The integrand is z dependent due to the inhomogeneous distribution of solvent close to the interface.

A look at the different contributions to the free energy shows that the intermolecular repulsive interactions have not been taken into account. To this end, we introduce packing constraints that are z -dependent due to the inhomogeneous distribution of solvent and polymer segments along the z direction. The constraint reads

$$\langle \phi_p(z) \rangle + \langle \phi_s(z) \rangle = \sigma l^3 \langle n(z) \rangle + \langle \phi_s(z) \rangle = 1 \quad \text{for all } z \quad (3)$$

where the first term is the volume fraction of polymer at distance z , and the second is the volume fraction of solvent at z .

In order to minimize the free energy density (1) with respect to the *pdf* of chain conformations and solvent density profile, subject to the packing constraint (3), we introduce a set of Lagrange multipliers $\pi(z)$. This yields for the *pdf*

$$P(\alpha) = \frac{1}{q} \exp \left[-\beta l^3 \int \pi(z) n(\alpha, z) dz - \beta \epsilon_{intra}(\alpha) - \beta \int_0^\delta n(\alpha, z) \chi_{s-p} dz - \beta \sigma l^2 \int \int \chi(|z - z'|) n(\alpha, z) \langle n(z') \rangle dz dz' \right] \quad (4)$$

q is a normalization constant ensuring $\sum_\alpha P(\alpha) = 1$ and $\beta = 1/k_B T$. Similarly, the solvent density profile is given by

$$\langle \phi_s(z) \rangle = e^{-\beta l^3 \pi(z) - \beta \mu_s} \quad (5)$$

where μ_s is the chemical potential of the solvent molecules and it is constant at all z .

The only unknowns needed to determine the *pdf* and the solvent density profile are the Lagrange multipliers $\pi(z)$. They are obtained by substituting the functional forms, Eqs. (4,5), into the constraint equation (3). In order to solve these equations, it is convenient to discretize space into a set of parallel layers converting the integral equations into a set of non-linear coupled equations. The details of the calculation can be found in Ref. [8].

The physical meaning of the Lagrange multipliers can be seen from Eq. (5). These quantities are related to the osmotic pressure necessary to keep the chemical potential of the solvent constant at all z . Furthermore, they represent the effective repulsive interactions (lateral pressure) between the polymer that force the chains to stretch out from the surface into the bulk solution.

In order to compare the predictions of the theory with the experimental pressure-area isotherms we need to derive theoretically the lateral pressure. This is obtained by a differentiation of the total free energy W with respect to the total area A , i.e.

$$\Pi = - \left(\frac{\partial W}{\partial A} \right)_{N,T} \quad (6)$$

Taking the derivative of the free energy (1), after substituting the *pdf* and the solvent density profiles, Eqs. (4,5), yields the following surface pressure

$$\beta \Pi = \sigma + \int \beta \pi(z) dz - \sigma N + \frac{1}{2l^4} \int \int \beta \chi(|z - z'|) \langle \phi_p(z) \rangle \langle \phi_p(z') \rangle dz dz' \quad (7)$$

where N is the tethered polymer chain length (either the PS or PEO blocks). The lateral pressure is readily calculated once the Lagrange multipliers are determined.

B. SCMF Parameters

The determination of the osmotic pressure profile $\{\pi(z)\}$ requires the solution of the constraint equations. The needed parameters are: (i) the surface density of polymer σ (or equivalently, the area per chain, $\Sigma = 1/\sigma$), (ii) the strength of the polymer-polymer attraction, $\chi(|z - z'|)$ (or, alternatively, the Lennard-Jones potential strength), (iii) the strength χ_{s-p} and the width δ of the polymer-interface interaction range, and (iv) the set of single chain conformations of the polymer under study.

We have chosen to use the rotational isomeric state model for the polymer chains. For both types of chains, PS and PEO, each segment is modeled as having three possible states. The three states are taken to be iso-energetic and each segment represents a styrene or an ethylene oxide (EO) monomer. The internal structure of the monomers, i.e., detail chemical structure and internal energy of the different states, is replaced by an effective monomer length representing the bond between the neighboring monomers. The length of the segments is $l_s = 4\text{\AA}$ and $l_{EO} = 3\text{\AA}$ for the styrene and EO units, respectively. Note that these values compare reasonably well with the proper length of the chemical segments in each type of polymer.

The constraint equations are solved by discretizing space into parallel layers of thickness $\delta = 1.84 l_{EO}$. This value of δ has been found to be the more convenient in the calculation, however the predictions of the theory are independent of the choice of δ [8]. This transforms the integral equations, Eq. 4, into a set of non-linear equations which are solved by standard numerical methods. We remark that once the set of single chain conformations is generated, it is used for all the calculations for different surface coverages and conditions. Further technical details of the calculations can be found in Ref. [8].

The values of the parameters defined above have not been optimized in order to obtain the best possible agreement with experiment. They were simply chosen on the basis of reasonable physical values. The value of the Lennard-Jones strength is $0.33k_B T$ for the styrene-styrene and $0.9k_B T$ for the EO-EO attractions, respectively. The only parameter whose value is not known experimentally is the EO-interface attraction parameter, χ_{s-p} . A few values of this parameter have been checked (in steps of $0.5 k_B T$). The one we finally used, $\chi_{s-p} = -1.0k_B T$, fits best the experimental data. We remark that even better agreement with the experimental observations can be achieved by further optimization of the parameters, but this is left to future studies.

IV. EXPERIMENTAL OBSERVATIONS AND THEORETICAL RESULTS

A. Isotherms and the PEO Layer Structure

On Fig. 1 we plot the experimental isotherms corresponding to different PEO chain lengths while keeping the length of the PS block fixed at $N_{PS} = 31$ (in one case $N_{PS} = 30$). A pseudo-plateau in the pressure-area isotherms can be seen in Fig. 1 signaling a small pressure variation over a large change in the area per molecule (Σ), especially for the longer chain lengths. This is in accord with previous experiments of Ref. [25]. The pressure-area isotherms in the plateau and the highly compressed regions are completely reproducible, for both compression and decompression cycles as has been already discussed in Ref. [25].

Hysteresis effects are observed only for the diluted region. Furthermore, for monolayers spread out at molecular areas a little bigger than the plateau values, the first compression is different from the following ones. For such a deposition we suspect that the chains are entangled at the surface without being able to disentangle during experimental times. Another problem with deposition done for Σ close to the plateau value is the appearance of two plateaus instead of one. For this reason, all experiments have been performed after spreading out the monolayer at very low pressure (and high Σ). The pressure isotherms have been always measured while compressing the monolayer. A hysteresis is still present under these conditions and leads to smaller pressures at large molecular areas during decompression. This could be explained by pre-orientation during the decompression: the entanglement of the chains at the interface is less pronounced when a polymer “brush” is decompressed than when it is compressed from a two-dimensional monolayer. Hence, it leads to smaller surface pressures in the former case.

Figure 2 shows the prediction of the SCMF theory together with the experimental pressure-area isotherms. As the SCMF method is limited by chain length of about 200 monomers, we show isotherms for three different chain lengths up to this value. The theory is in very good agreement with the experimental observations. The presence of the plateau is a manifestation of the preferential adsorption of the EO monomers at the air-water interface, as earlier suggested by Bijsterbosch et al. [25].

In order to obtain quantitative agreement between the measured isotherms and the theoretical findings it is necessary to take into account the role of the PS block (see Sec. IV.B below). The short PS block resides on the air side of the interface, is not attracted to the air-water interface and has strong attractive interactions with monomers of its own

type. Namely, the PS is in a poor solvent conditions (the poor “solvent” being the air). In addition, the strength of the attraction between the EO monomers and the interface is found to be considerably larger than the estimates given by Bijsterbosch et al. [25]. The value for χ_{s-p} we used and which fits the experiments is about $-k_B T$ per monomer. We have also performed calculations for bigger values of the EO-interface attraction in order to check if there is a first-order phase transition as predicted by Ligoure for long polymer chains [17]. However, our calculations as applied to intermediate chain lengths, do not show any indication of such a first-order transition even for attractions per monomer as strong as $\chi_{s-p} = -4k_B T$.

As the monolayer is compressed, starting from very large Σ , the isotherm shows a relatively sharp increase of pressure as Σ is decreased, followed by a plateau. The term “plateau” is loosely used hereafter (and by others) to denote a region for relatively small Σ where the pressure reaches a pseudo-plateau and increases only gradually as the layer is compressed. Upon even further compression, there is a very large increase of the pressure. This is due to the very large densities of the chains at small Σ resulting in very high pressures for all types of solvent qualities.

The understanding of the origin of the plateau is intimately related to the structural behavior of the polymer layer as a function of the area per molecule. We consider only the PEO part of the layer which is responsible for the presence of the plateau and for the overall shape of the isotherm. The PS block “tunes” the pressure in the different regimes but does not change the qualitative shape of the isotherms (see Sec. IV.B below).

Figure 3 shows the pressure as a function of Σ (the area per molecule) and $\langle\phi_p(z)\rangle$, the density profiles of the PEO chains, for four different surface densities, as calculated from the SCMF theory. The density profile at large Σ corresponds to distances between tethering points larger than the radius of gyration of the chain. The density profile reveals that at these large Σ values, the PEO chains form a quasi two-dimensional layer at the air-water interface due to the strong monomer-interface attraction.

Up to the onset of the plateau in the pressure-area isotherm, as Σ is decreased, the density profile looks very similar to the very dilute case. Namely, down to the plateau region of the isotherm, the PEO forms a quasi two-dimensional layer. Comparison of the increase of the pressure with surface density in this low density region (high Σ) with that of non attracting surfaces reveals that the increase in the former case is much sharper than in the non-attracting case. The reason is that when the monomers are attracted by the interface, their local density becomes higher resulting in larger lateral monomer repulsion and hence larger pressure. This is to be contrasted with non-attractive interfaces where the chains stretch quite substantially into the bulk solution (the “mushroom” regime).

The appearance of the plateau in the pressure-area isotherm corresponds to the point where the density profile shows that a high fraction of the PEO monomers is adsorbed on the surface. Another feature of this plateau, as seen from the density profiles, is the appearance of a second structure reminiscent to a brush composed of chains with the same number of segments as the PEO chains but without the ones attracted to the surface. This shape of the profile remains basically the same as Σ decreases. Upon further compression, the brush-like part of the profile corresponds to effective longer chain lengths because the polymer density at the interface does not change.

The formation of the adsorbed layer at low surface coverages implies that for this region the pressure should exclusively be determined by the number of segments in the layer. Therefore, the pressure should scale with Σ/N_{PEO} . Figure 4 shows that for all Σ values higher then the onset of the plateau, the pressure scale reasonable well with Σ/N_{PEO} both as measured experimentally for $N_{\text{PS}} = 30$ (4a) and from the SCMF calculation (4b). In addition, it was checked experimentally for isotherms with $N_{\text{PS}} = 13$ and 43.

Clearly, once the brush appears the pressure shows a behavior combining the highly dense adsorbed layer one with that of the short chain length brush. Empirically, we find that in the high surface coverage regime the calculated pressure scales with $\sigma(N_{\text{PEO}})^{0.6}$ as shown in Fig. 5. However, as discussed in detail in Refs. [29,8], special care is needed in trying to describe these polymer layers with scaling concepts since the chain length are too short and there is no easy definition of the scaling regimes such as the “mushroom” and “brush” regimes.

From the experimental observations and the SCMF predictions we find that the width of the plateau region increases with the size of the PEO chain, while the height of the plateau is independent of N_{PEO} and is equal to about 10 mN/m. The height of the plateau is a function of the PS chain length (see below) and from the SCMF calculations (not shown) it also depends on the affinity of the interface to the EO monomers (our χ_{s-p} parameter).

Figure 6 shows the PEO contribution to the pressure Π , and the square of the volume fraction of the adsorbed layer $\langle\phi_p(1)\rangle^2$, including segments at distances $0 \leq z \leq \delta$ from the surface, as a function of Σ/N_{PEO} , as calculated from the SCMF theory. For Σ higher than the onset of the plateau, the square of the volume fraction of the adsorbed layer is identical in shape, and, therefore, fully determines, the pressure of the PEO layer. This is again a manifestation of the quasi two-dimensional behavior of the PEO layer up to the onset of the plateau. For higher surface densities (lower Σ), the polymer layer starts to behave like a combination of a 2d layer and a brush. Hence, there is no reason there why Π and $\langle\phi_p(1)\rangle^2$ will be proportional.

B. The Effect of PS Block

The effect of the PS chain length, N_{PS} , on the pressure-area isotherms are presented in Fig. 7a for the experimental isotherms and in Fig. 7b for the SCMF predictions. As explained above, the pressure isotherms are more conveniently plotted as a function of Σ/N_{PEO} . We first note that the dependence of the isotherms on N_{PS} is rather small for Σ values higher than the plateau region. However, When N_{PS} increases, the height and the slope of the plateau decreases. The experimental isotherm of a pure PEO homopolymer is plotted (triangles) on the same figure for comparison. For the latter, a plateau is observed as well but at a lower surface pressure. There is no steep rise in the pressure at small molecular area because the absence of an anchoring hydrophobic block. Instead the pure PEO layer loses its stability.

For very short PS chains, the PS block may be thought of as being in a liquid “collapse” state (bad solvent conditions). In fact, to the best of our knowledge, no previous measurements exist for the glass transition temperature, T_g , of PS in a diblock copolymer confined to a two-dimensional surface. In bulk (three-dimensional) systems, T_g is equal to 23°, 67° and 76° C, respectively for $N_{\text{PS}} = 13, 30$ and 43. Careful surface viscosity experiments are needed in order to further clarify this point.

The SCMF results shown in Fig. 7b are in good agreement with the experimental observations on the effect of the PS block. The PS block is modeled in the theory as being in poor solvent conditions so that without being linked to the PEO block, the PS layer would undergo a two dimensional “gas-liquid” (collapse) phase transition. However, the presence of the attached PEO block (for which the water is a good solvent), ensures that the PS layer is stable for all surface coverages down to very compressed states.

C. Mean-Field Theory: Dilute Region

In order to complement the numerical and more quantitative results of the SCMF theory, a simple mean-field approach is proposed. Although it is more qualitative, it offers a simple explanation of the PS-PEO isotherms for the dilute regime and is in semi-quantitative accord both with the experiments and the SCMF approach.

Based on the experimental isotherms and SCMF polymer profiles, we model the polymer layer in the dilute region of the isotherm (Σ larger than the plateau value), as a polymer layer where N_2 monomers of each PEO chain form an effective 2d layer whose thickness does not vary upon compression. Since we expect $N_2 \approx N_{\text{PEO}}$ for densities smaller than the 2d overlap density, the effect of the other PEO monomers which do not participate in the 2d layer ($N_{\text{PEO}} - N_2$ per chain) is neglected. On the other hand, the attraction of the PEO monomers to the air-water interface plays an important role in the 2d behavior of the PS-PEO copolymer layer.

Let us first consider the thermodynamics of a 2d PEO layer without the effect of the PS chains. They will be included later. The free energy of mixing can be written as a 2d Flory-Huggins free energy in terms of the area fraction occupied by the PEO monomers on the surface: $\phi_2 = l^2 N_2 \sigma = l^2 N_2 / \Sigma$. This area fraction corresponds to the volume fraction of the polymer chains in the first layer, $\langle \phi_p(1) \rangle$ as was defined earlier (Sec. III.A).

$$F_{\text{site}} = \frac{l^2}{A} W = k_B T \left[\frac{\phi_2}{N_2} \ln \phi_2 + (1 - \phi_2) \ln(1 - \phi_2) \right] + \chi_0 \phi_2 (1 - \phi_2) + \chi_{s-p} \phi_2 \quad (8)$$

where $l = l_{\text{EO}} \simeq 3\text{\AA}$ is the EO monomer size. The first two terms are just the entropy of mixing of the PEO monomers at the interface, the third term is the enthalpy of mixing, and the last term represents the attractive surface interaction of the PEO monomers with an interaction parameter χ_{s-p} varying between $-0.5k_B T$ and $-1.0k_B T$.

The PS block is anchored at the surface on the air side. As air acts as a bad solvent for the relatively short PS chains, the chains can be considered to be in a collapse state, each occupying an area $\Sigma_{\text{PS}} = (N_{\text{PS}})^{2/3} l_s^2$ which is estimated around $\Sigma_{\text{PS}} \simeq 150 - 200\text{\AA}^2$ for $N_{\text{PS}} \simeq 30 - 40$ and the PS monomer size is taken as $l_s = 4\text{\AA}$. We take into account two effects of the PS block on the PEO chains. First, the area available for the PEO monomers is reduced. The available area per PEO chain is only $\Sigma - \Sigma_{\text{PS}}$. Second, we take into account the attractive PS-PS interactions.

Altogether the more general free energy (per site) is

$$F_{\text{site}} = k_B T \left[\frac{\phi_2}{N_2} \log \phi_2 + (1 - \phi_2) \log(1 - \phi_2) \right] + \chi_0 \phi_2 (1 - \phi_2) + \chi_{s-p} \phi_2 + \chi_1 \phi_{\text{PS}} (1 - \phi_{\text{PS}}) \quad (9)$$

where

$$\phi_{\text{PS}} = \Sigma_{\text{PS}} / \Sigma \quad \phi_2 = l^2 N_2 / (\Sigma - \Sigma_{\text{PS}}) \quad (10)$$

The surface pressure can be calculated by differentiating the total free energy $W = AF_{\text{site}}/l^2$ with respect to the total surface area A . Alternatively, the surface pressure Π can be obtained directly from the free energy density F_{site} , yielding

$$\Pi = -\frac{1}{l^2} \frac{\partial(\Sigma F_{\text{site}})}{\partial \Sigma} = -\frac{1}{l^2} (F_{\text{site}} + \Sigma \frac{\partial F_{\text{site}}}{\partial \Sigma}) \quad (11)$$

By estimating the values of the parameters: N_2 , χ_0 , χ_1 , Σ_{PS} and χ_{s-p} , we can obtain $\Pi(\Sigma)$ from Eqs. (9)-(11). However, we present here only the analytical expansion of the pressure Π in powers of Σ^{-1} valid for the dilute limit, $\Sigma \gg \Sigma_{\text{PS}} \simeq 200\text{\AA}$. Neglecting the entropy of the PEO chains (since $1/N_2$ is rather small) and expanding Eq. (9) we get

$$\frac{F_{\text{site}}}{k_B T} \simeq (-1 + \beta\chi_{s-p} - \beta\chi_0)\phi_0 + (-1 + \beta\chi_{s-p} + \beta\chi_0)\phi_0\phi_{\text{PS}} + \frac{1}{2}(1 - 2\beta\chi_0)\phi_0^2 + \beta\chi_1\phi_{\text{PS}} - \beta\chi_1\phi_{\text{PS}}^2 \quad (12)$$

where $\phi_0 = l^2 N_2 / \Sigma$ is the unperturbed PEO area fraction without the effect of the PS block and $\beta = 1/k_B T$. The pressure is readily calculated from (12) to be

$$\frac{l^2}{k_B T} \Pi \simeq \left[(-1 + \beta\chi_{s-p} + \beta\chi_0) \frac{\Sigma_{\text{PS}}}{l^2 N_2} - \beta\chi_1 \left(\frac{\Sigma_{\text{PS}}}{l^2 N_2} \right)^2 + \frac{1}{2} - \beta\chi_0 \right] \phi_0^2 \quad (13)$$

Taking the following estimates for the parameters: $\chi_0 \simeq 0$, $\Sigma_{\text{PS}}/l^2 N_2 \simeq l_s^2 N_{\text{PS}}^{2/3}/l^2 N_2 \simeq 0.1$, we get the following estimate of the leading term in the pressure as function of the surface coverage $\sigma = 1/\Sigma$

$$\frac{\Pi}{k_B T} \simeq \left[\frac{1}{2} - 0.1(1 - \beta\chi_{s-p}) - 0.01\beta\chi_1 \right] (N_2 l \sigma)^2 \quad (14)$$

From (14) we see that the interaction effect of the PS monomers is rather small (for the dilute regime). For reasonable estimates of the PEO-surface interaction parameter $\beta\chi_{s-p} \simeq -1.0$ we get that the pressure depends on $(N_2 l \sigma)^2$ with a prefactor of 0.3. This result is in accord with the SCMF calculation presented on Fig. 6 where it is seen that indeed $\Pi \sim \phi_2^2 \sim (\sigma N_2)^2$ for all dilute surface densities till the plateau. Note that ϕ_2 as was defined in this section corresponds to $\langle \phi_p(1) \rangle$ of the SCMF calculations. Hence, the simple calculation presented in this section gives a simpler description (albeit more approximated) to the thermodynamics of the PS-PEO layer for compression till the plateau values. We note again that the PEO effective size is taken as N_2 and includes only those PEO monomers that lie on the 2d surface.

Equations (13)-(14) can be compared with the experimental isotherms. To do so we plot the experimental isotherms Π/N_{PEO}^2 as a function of $1/\Sigma^2 = \sigma^2$ for the various PS-PEO copolymers. For surface densities smaller than the plateau values, we observe the expected linear dependence for all our copolymer systems. From the slope given by (14) $0.3l^2 N_2^2 / (k_B T N_{\text{PEO}}^2)$, the fraction of the PEO monomers adsorbed at the interface is deduced assuming that the size of a PEO monomer is $l = 3\text{\AA}$.

On Fig. 8, the variation of this fraction N_2/N_{PEO} is presented as a function of the chain length N_{PEO} . For short chains, the fraction of monomers adsorbed at the interface is less than one and increases with N_{PEO} . It reaches an asymptotic value for the longer chains. Note that this asymptotic value is larger than one, due probably to the approximations used in determining the prefactor. We can consider that part of the PEO monomers are constrained by their link to the PS block and effectively are shielding this block from a unfavorable contact with the water. The total number of monomers affected by this constraint should be independent of the length of the PEO chain. Consequently, their ratio to the total chain length should decrease with N_{PEO} and will be negligible for the long chains.

V. SUMMARY

The structure and thermodynamics of PS-PEO layers have been studied using a combination of experimental observations, molecular theory (SCMF) and a simple mean-field approach. The picture that emerges is that at low surface coverages the PEO forms a two dimensional layer due to the attractions of the EO segments to the air-water interface. This can be understood since the ethylene oxide monomer shows amphiphilic (surface activity) behavior. Upon further compression, the adsorbed polymers start to overlap and there is a plateau in the pressure isotherms. The plateau corresponds to the region where there is a 2d layer of constant density of ethylene-oxide and a water soluble brush-like layer. At very high surface densities the pressure increases very sharply due to the strong repulsion

between the stretched and adsorbed parts of the layer. The PS block is in a poor solvent environment, hence being in a collapsed state at all surface coverages.

The most important difference between the PS-PEO and other block copolymer systems is the attraction of the EO monomers to the interface. The ramifications of this EO attraction to hydrophobic surfaces is very important in the understanding and design of biocompatible materials and polymer decorated liposomes.

The structural changes of the PEO layer are the result of the competition between the solubility of the EO monomers in water and their favorable energy of interaction with the interface. This energy is estimated from the SCMF to be or order of one $k_B T$. This indicates that the PEO layer cannot be treated within the general framework of “mushrooms” and “brush” regimes usually considered for layers of tethered and long polymers. A theoretical description of this layers requires the explicit consideration of the 2d EO layer formed at the interface for all polymer surface coverages.

The role of the PS block is to anchor the polymer to the interface and to tune the values of the pressures, i.e. the height of the plateau region. This is because the chain lengths of the PS blocks studied here are short enough, as compared to the PEO block, such that the overall behavior of the layer is determined by the water soluble block (PEO).

Acknowledgments

One of us (IS) wishes to acknowledge support from the NSF under grant No. CTS-9624268, while DA acknowledges support from US-Israel Binational Foundation (BSF) under grant No. 94-00291. IS is a Camille Dreyfus teacher-scholar.

-
- [1] G. L. Gaines, *Insoluble monolayers at liquid-gas interfaces* (Interscience, New York, 1966).
 - [2] A. W. Adamson, *Physical chemistry of surfaces* (Wiley, New York, 1990).
 - [3] *Micelles, membranes, microemulsions, and monolayers*, Edited by D. Roux, W. M. Gelbart, and A. Ben-Shaul, (Springer-Verlag, New York, 1994).
 - [4] S.T. Milner, *Science*, **251**, 905, 1991.
 - [5] A. Halperin and M. Tirrell and T. P. Lodge, *Adv. Pol. Sci.* **100**, 31 (1991).
 - [6] A. Halperin, in *Soft Order in Physical Systems*, Nato ASI Series, Vol. 323, Eds. Y. Rabin and R. Bruinsma (Plenum, New York, 1994), pg. 33.
 - [7] Gary S. Grest and Michael Murat, in *Monte Carlo and Molecular Dynamics Simulations in Polymer Science*, edited by K. Binder, (Clarendon, Oxford 1995), pg. 476.
 - [8] I. Szleifer and M. A. Carignano, *Adv. Chem. Phys.* **XCIV**, 165 (1996).
 - [9] M. Adamuti-Trache, W. E. McMullen, and J. F. Douglas, *J. Chem. Phys.* **105**, 4798 (1996).
 - [10] P. Auroy, L. Auvray, and L. Léger, *Phys. Rev. Lett.* **66**, 719 (1991).
 - [11] P. Auroy, L. Auvray, and L. Léger, *Macromolecules* **24**, 2523 (1991).
 - [12] M. Stamm and J. R. Dorgan, *Coll. Surf. A* **86**, 143 (1994).
 - [13] J. Field, C. Toprakcioglu, R. Ball, H. Stanley, L. Dai, W. Barford, J. Penfold, G. Smith, and W. Hamilton, *Macromolecules* **25**, 434 (1992).
 - [14] S. K. Satija, C. F. Majkrzak, T. P. Russell, S. K. Sinha, E. B. Sirota, and G. J. Hughes, *Macromolecules* **23**, 3860 (1990).
 - [15] C. Amiel, M. Sikka, J. W. S. Jr., Y.-H. Tsao, M. Tirrell, and J. W. Mays, *Macromolecules* **28**, 3125 (1995).
 - [16] O. Guiselin, L. T. Lee, B. Farnoux, and A. Lapp, *J. Chem. Phys.* **95**, 4632 (1991).
 - [17] C. Ligoure, *J. Phys. II* **3**, 1607 (1993).
 - [18] M. Aubouy, O. Guiselin, and E. Raphael, *Macromolecules* **29**, 7261 (1996).
 - [19] V. Aharonson, D. Andelman, A. Zilman, P. A. Pincus, and E. Raphael, *Physica A* **204**, 1 (1994).
 - [20] M. S. Kent, L. T. Lee, B. J. Factor, F. Rondelez, and G. S. Smith, *J. Chem. Phys.* **103**, 2320 (1995).
 - [21] B. H. Cao and M. W. Kim, *Faraday Discuss.* **98**, 245 (1994).
 - [22] M. W. Kim and B. H. Cao, *Europhys. Lett.* **24**, 229 (1993).
 - [23] S. K. Gissing, R. W. Richards, and B. R. Rochford, *Coll. Surf. A* **86**, 171 (1993).
 - [24] R. W. Richards, B. R. Rochford, and J. R. P. Webster, *Faraday Discuss.* **98**, 263 (1994).
 - [25] H. D. Bijsterbosch, V. O. de Haan, A. W. de Graaf, M. Mellema, F. A. M. Leermakers, M. A. C. Stuart, and A. A. van Well, *Langmuir* **11**, 4467 (1995).
 - [26] J. M. Harris, *Poly(ethylene glycol) Chemistry. Biotechnical and Biomedical Applications* (Plenum Press, New York, NY, 1992).

- [27] I. Szleifer, Curr. Opin. Solid State and Mat. Science **2**, in press (1997).
- [28] *Stealth Liposomes*, Edited by D. D. Lasic and F. Martin (CRC Press, Boca Raton, FL, 1995).
- [29] M. A. Carignano and I. Szleifer, Macromolecules **28**, 3197 (1995).
- [30] I. Szleifer, Curr. Opin. Coll. Interface Sci. **1**, 416 (1996).
- [31] A. Ben-Shaul, I. Szleifer, and W. M. Gelbart, J. Chem. Phys. **83**, 3597 (1985).

TABLE CAPTION

Table 1 The different copolymers used in the isothermal measurements. N_{PS} is the number of PS monomers and N_{PEO} the number of PEO monomers. The copolymers labeled with D have a PS block which is partially deuterated.

FIGURE CAPTIONS

- Figure 1** Experimental surface pressure – area isotherms at $T = 18^\circ \text{C}$ of PS-PEO copolymers with several sizes of the PEO block and with the same PS block, $N_{\text{PS}} = 31$, beside one case with $N_{\text{PS}} = 30$. (We will ignore the difference between these two similar PS sizes).
- Figure 2** direct comparison of experimental pressure-area isotherms with those obtained from the SCMF theory, for three different copolymers: 30-179 (dotted line); 30-100 (dashed line); 43-64 (smooth line). The experimental curves are denoted by their data points (full circles) and are very close to the calculated ones.
- Figure 3** (a) Pressure isotherm as function of the surface density $\sigma = 1/\Sigma$; (b) density profiles $\langle \phi_p(z) \rangle$ as function of the distance from the air-water interface, z ; both obtained from the SCMF theory. Only the contribution of the PEO block is shown. The smooth, dotted, dashed and dashed-dotted lines in (b) corresponds, respectively, to the points marked as 1, 2, 3 and 4 on the isotherm in (a) having the surface density: 0.0012, 0.0006, 0.00038 and 0.00022 \AA^{-2} , respectively.
- Figure 4** (a) same as Fig. 1 but the data is plotted as a function of the area/molecule rescaled by the number of PEO monomers N_{PEO} : Σ/N_{PEO} . (b) The contribution of the PEO block to the pressure calculated from the SCMF theory as a function of the same rescaled area as in (a) for three PEO block sizes: $N_{\text{PEO}}=64$ (smooth line); 118 (dotted line); 179 (dashed line).
- Figure 5** Same values and symbols as for the isotherms in Fig. 4b but the isotherms here are plotted with a rescaled surface density, $(N_{\text{PEO}})^{0.6}/\Sigma$, in order to show the scaling behavior in the “brush” regime (high σ).
- Figure 6** Calculated contribution of the PEO block to the surface pressure (smooth line) and $25\langle \phi_p(1) \rangle^2$ (dotted line) as function of Σ/N_{PEO} for $N_{\text{PEO}} = 179$. The two curves become identical in the large Σ region (roughly for $\Sigma/N_{\text{PEO}} \geq 18 \text{ \AA}^2$) demonstrating that Π is proportional to $\langle \phi_p(1) \rangle^2$ in this region. This essentially two-dimensional behavior is expected for the dilute region.
- Figure 7** (a) Effect of N_{PS} , the size of the PS block, on the experimental measured pressure as function of Σ/N_{PEO} the rescaled area/molecule. (b) Calculation from the SCMF theory for $N_{\text{PS}} = 13$ (smooth line), $N_{\text{PS}} = 20$ (dotted line), $N_{\text{PS}} = 30$ (dashed line) and $N_{\text{PS}} = 50$ (long dashed line). In all calculated isotherms $N_{\text{PEO}} = 100$.
- Figure 8** Fraction of PEO monomers at the interface, N_2/N_{PEO} , as a function of N_{PEO} , the total PEO chain length. The value for large N_{PEO} is larger than one, probably because of the approximations in the prefactor in (14).

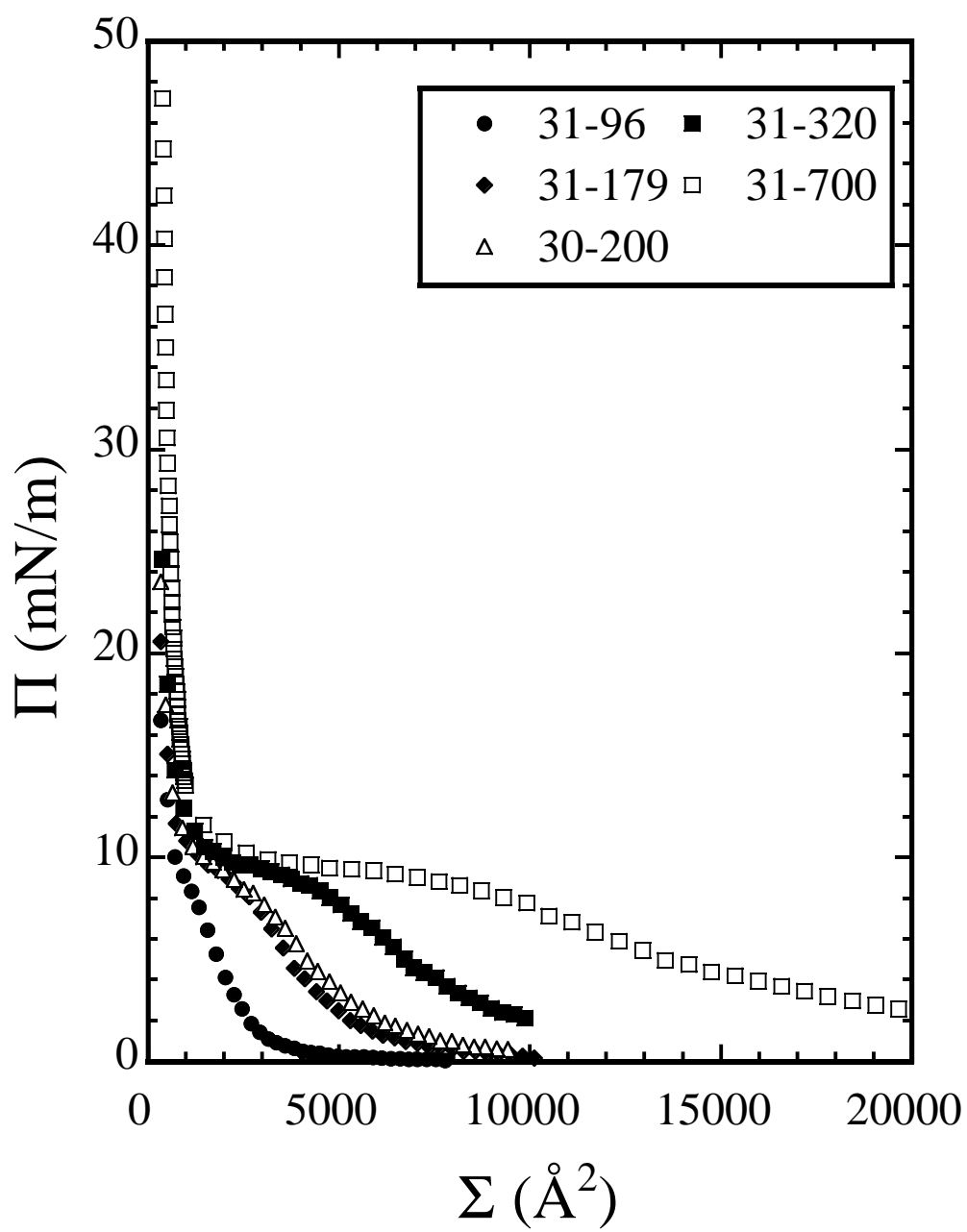


Fig. 1

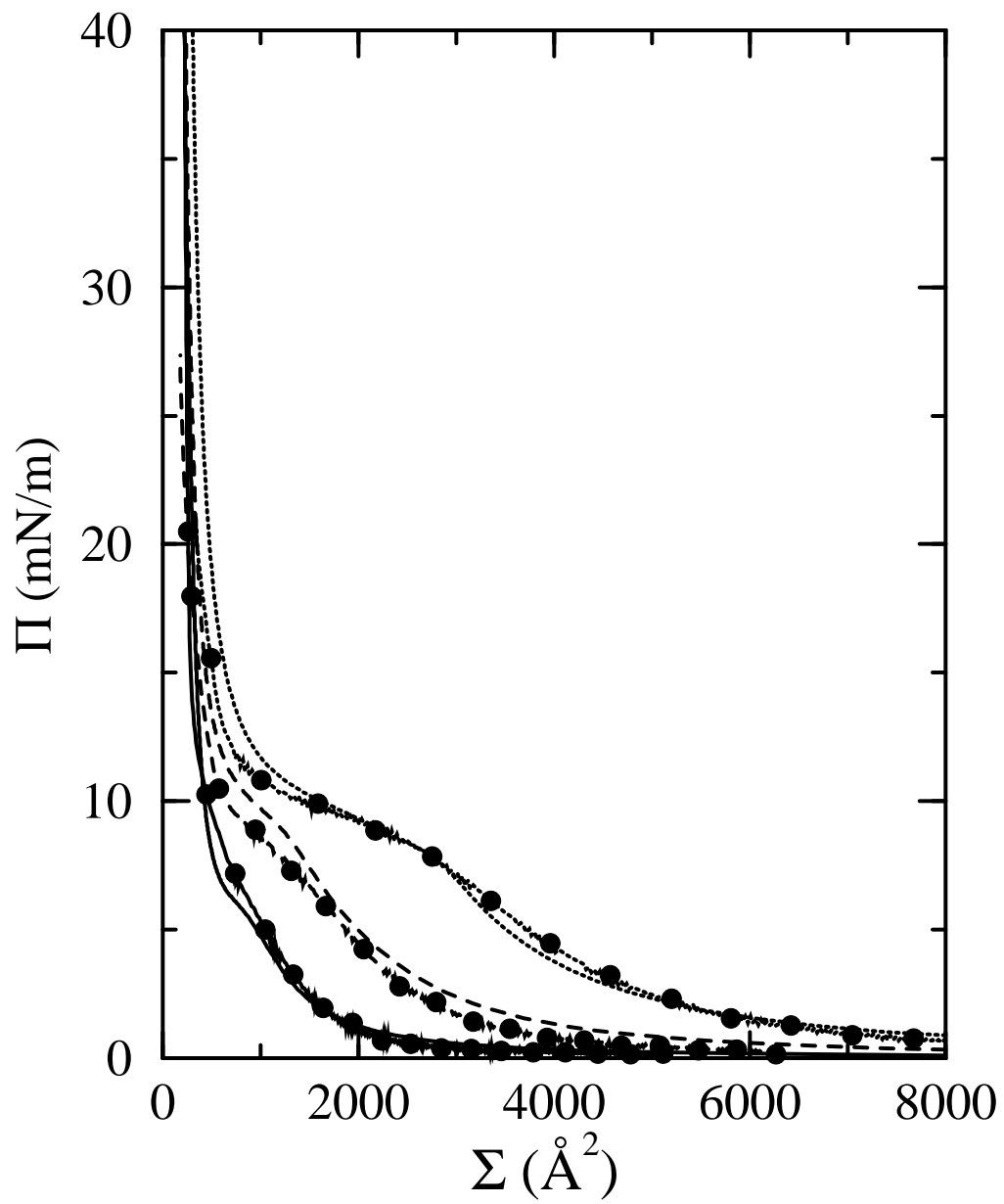


Fig. 2

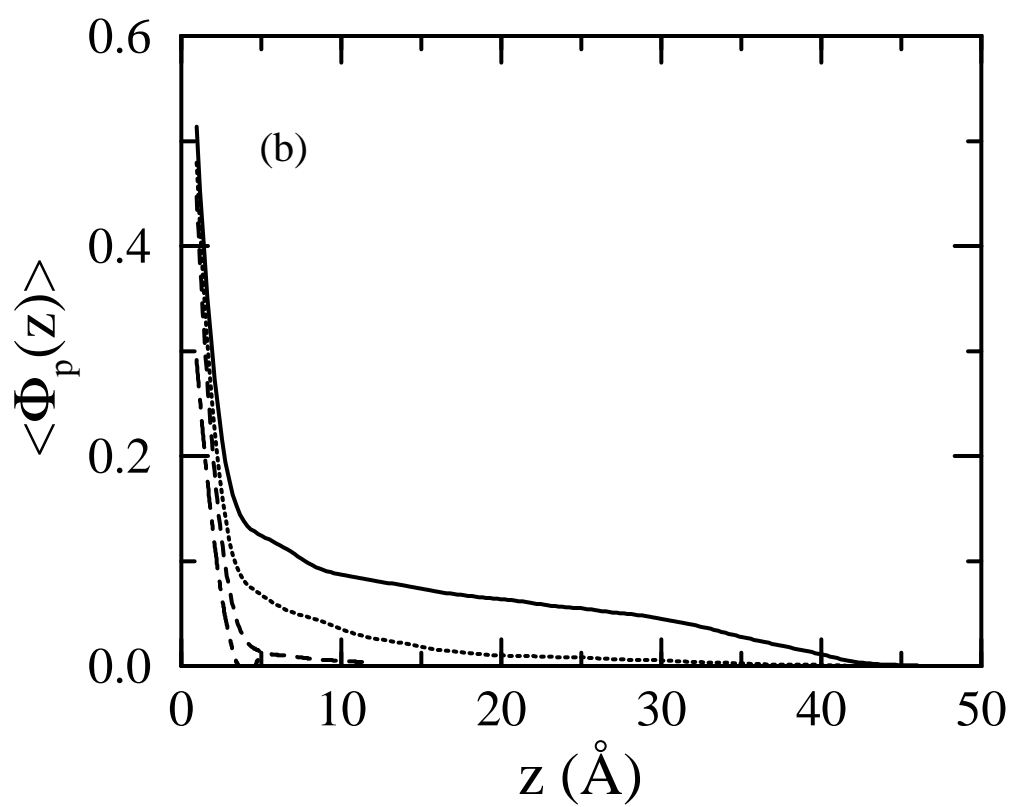
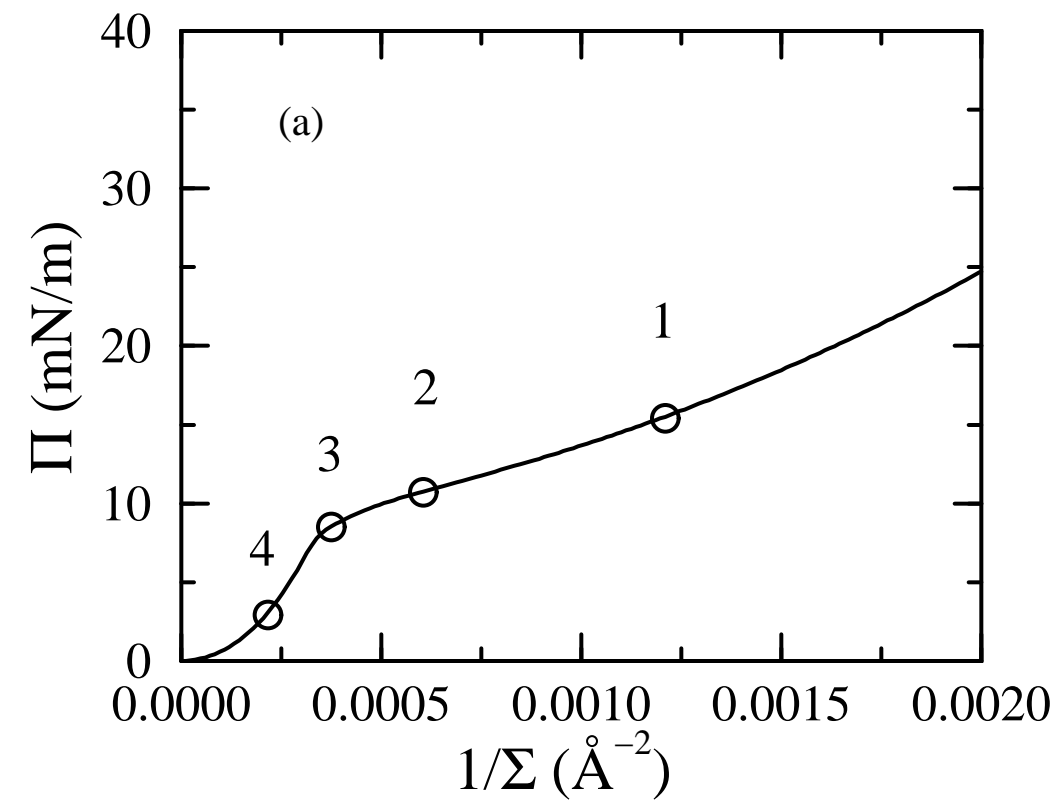


Fig. 3

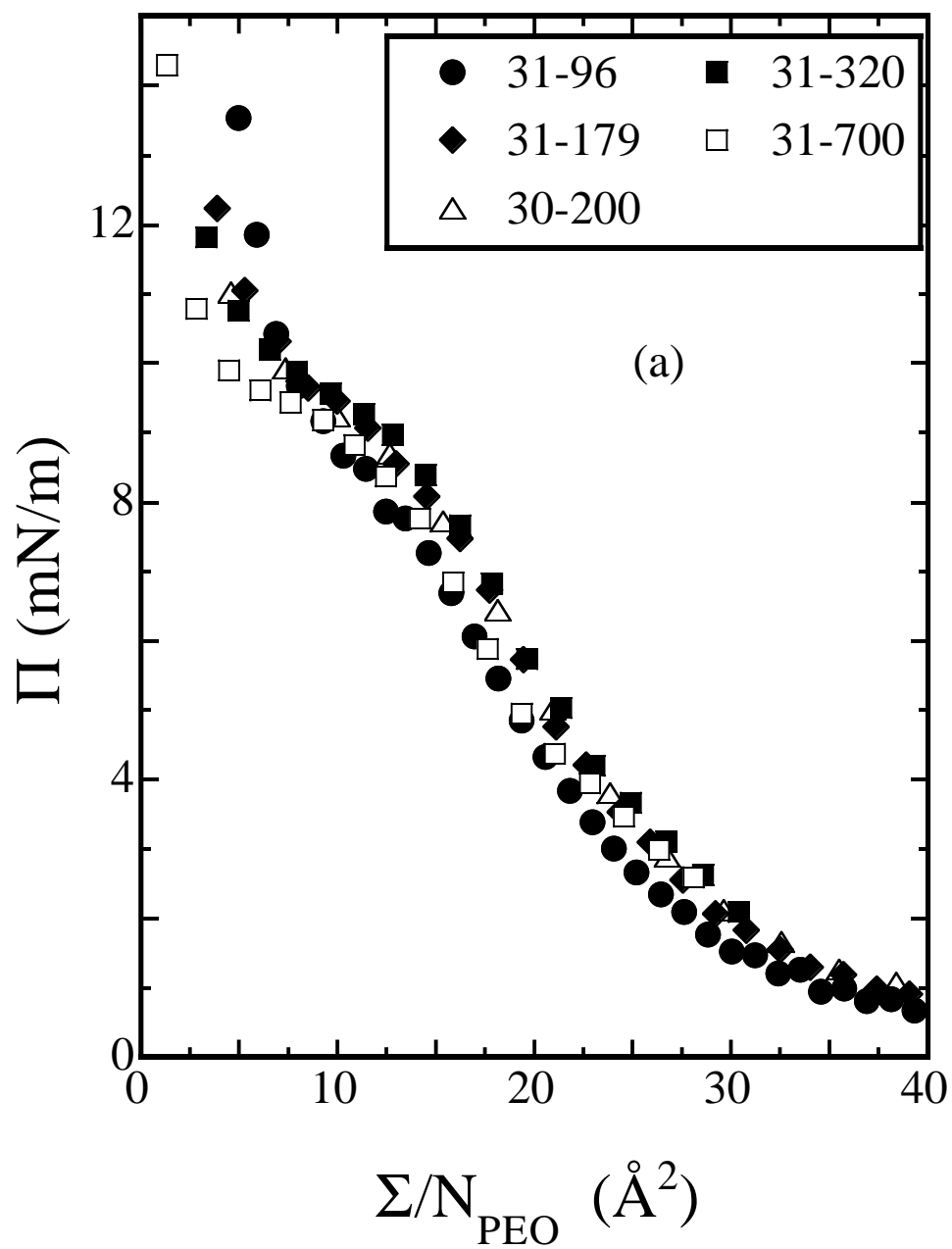


Fig. 4a

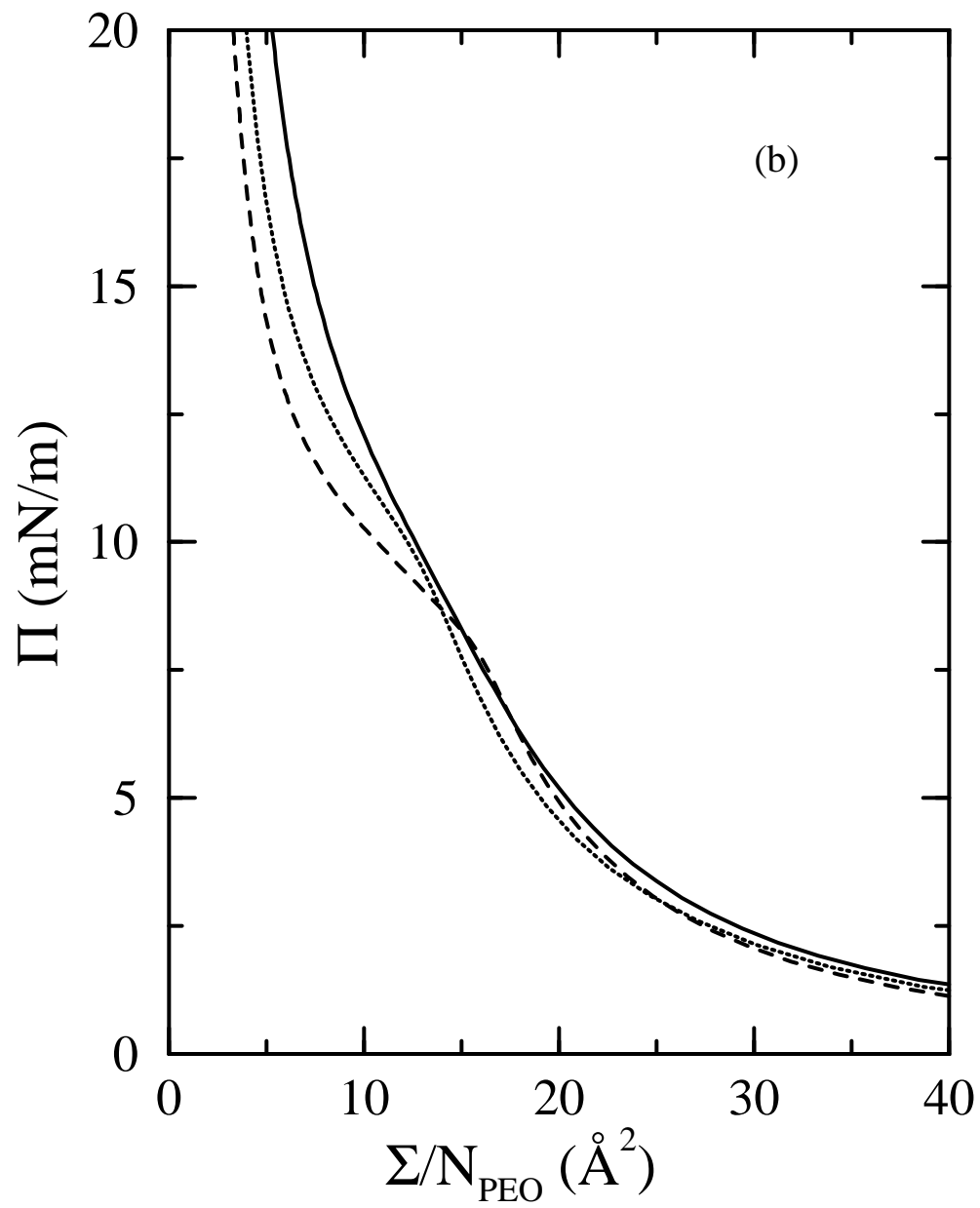


Fig. 4b

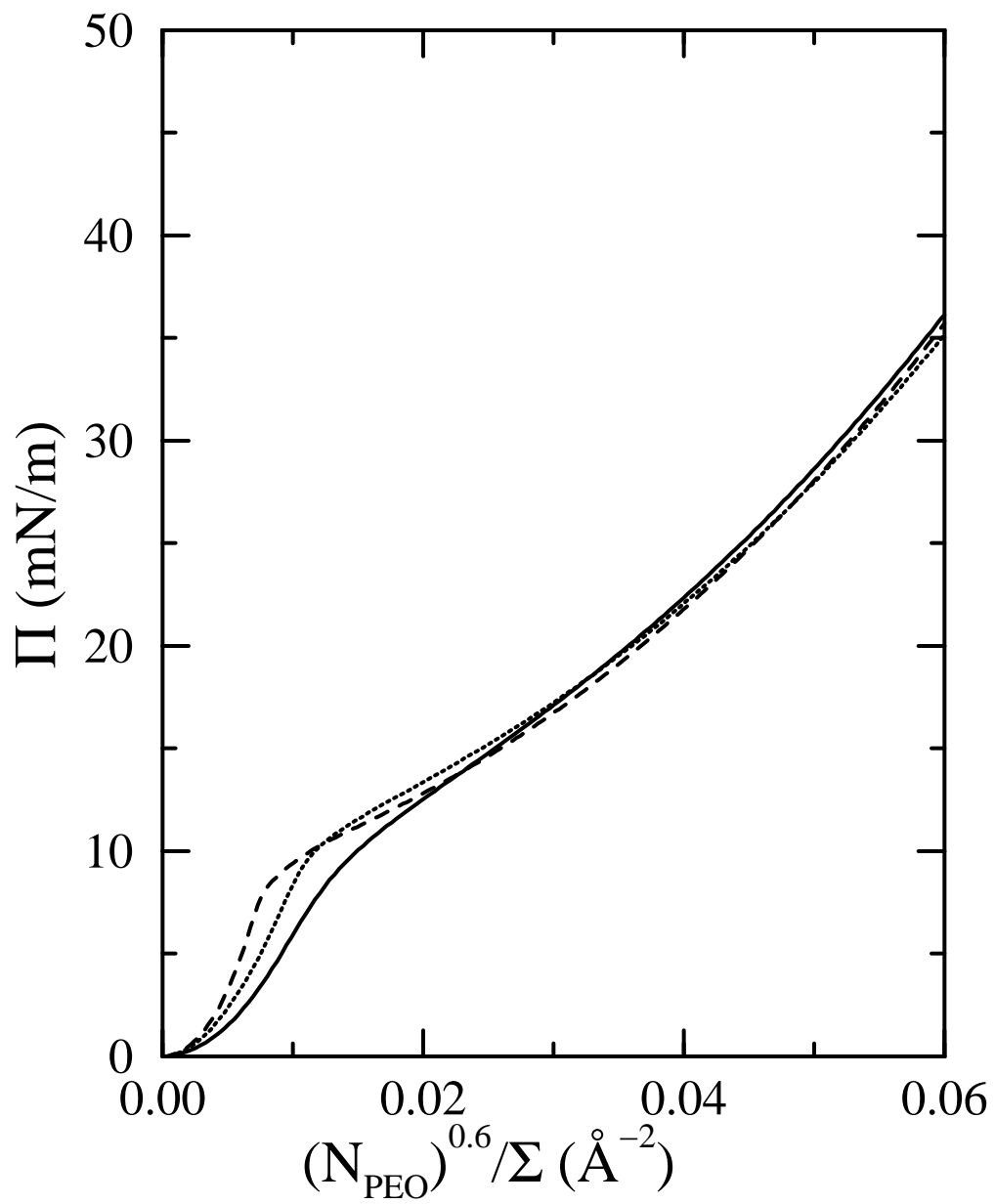


Fig. 5

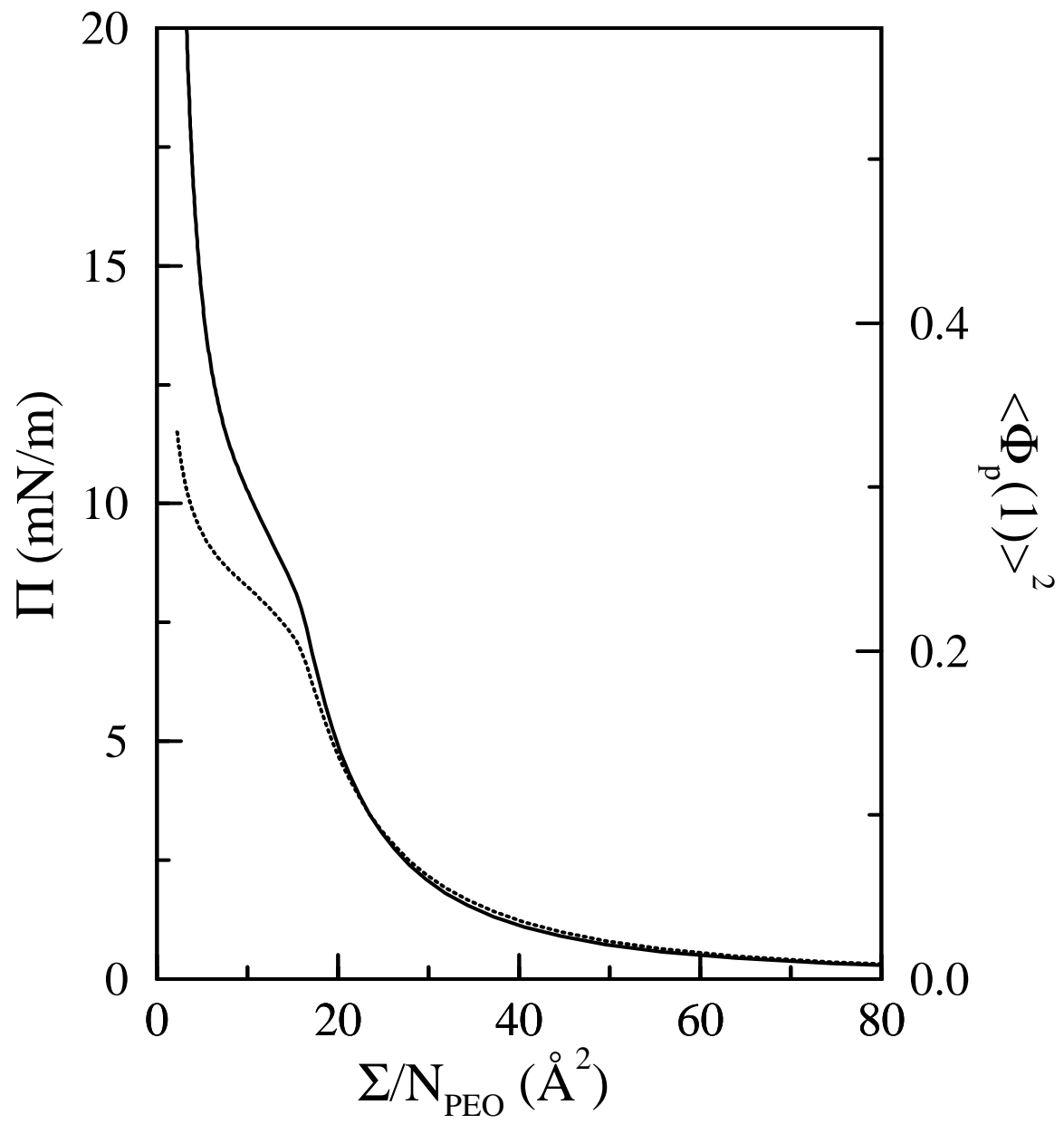


Fig. 6

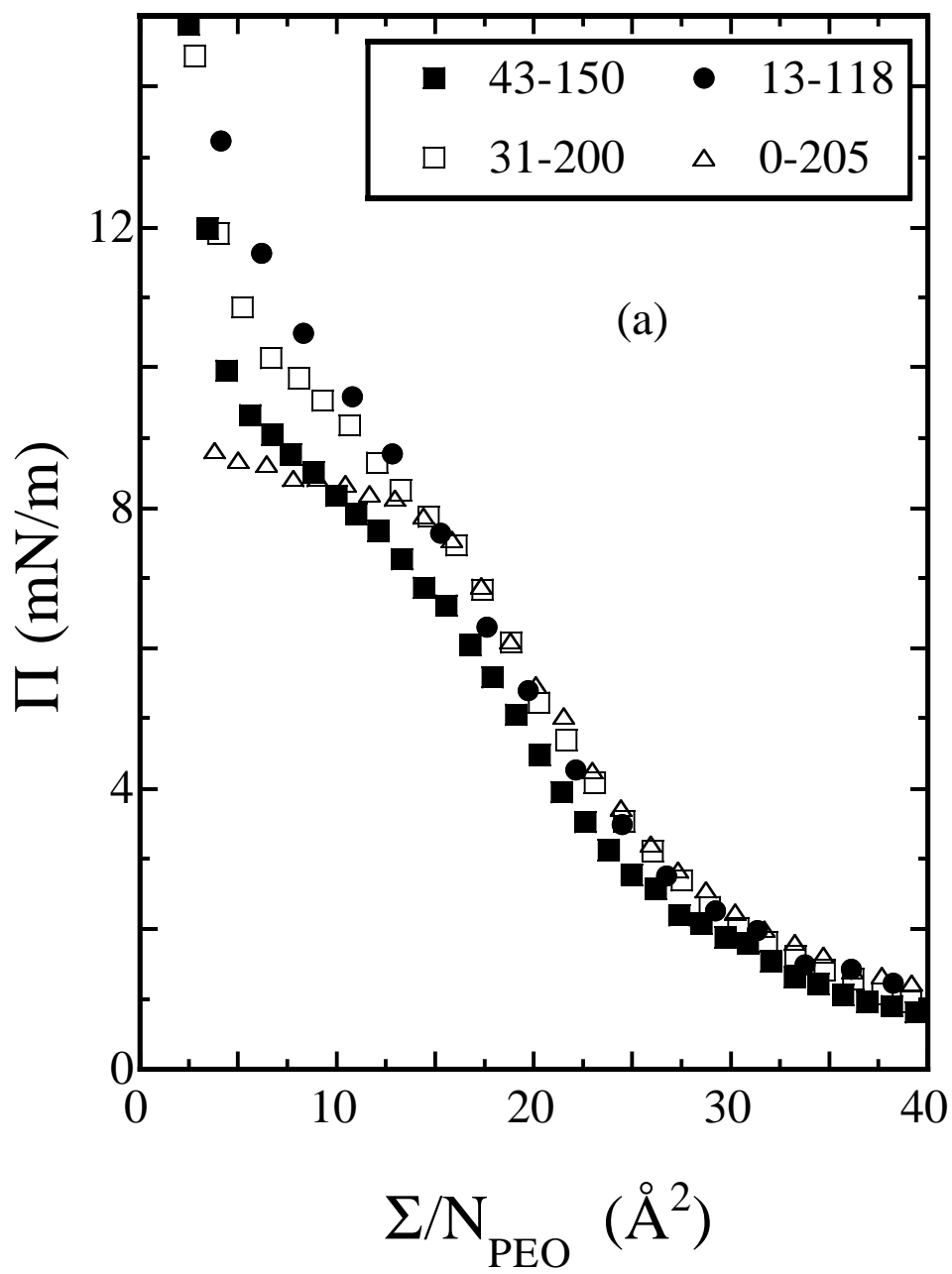


Fig. 7a

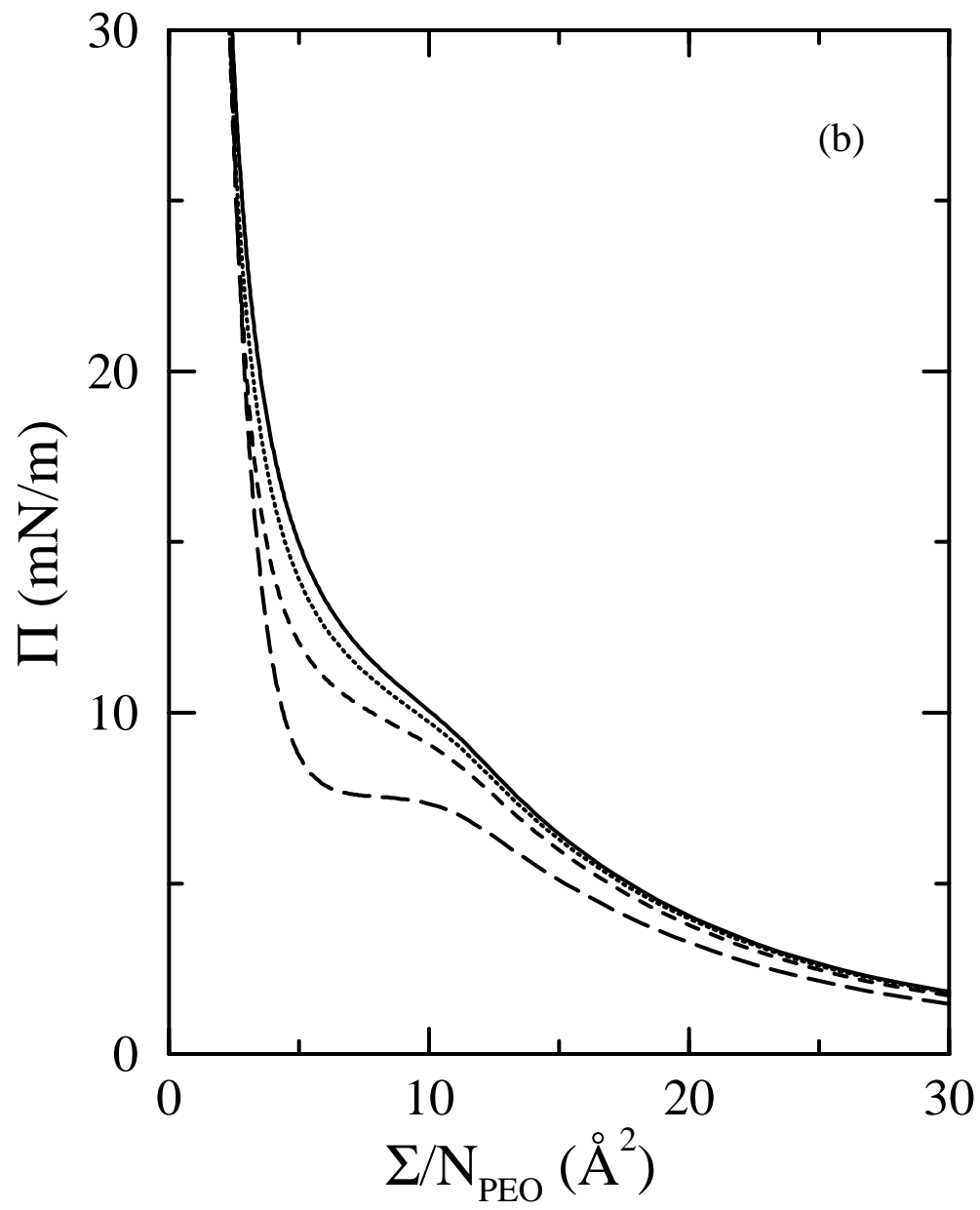


Fig. 7b

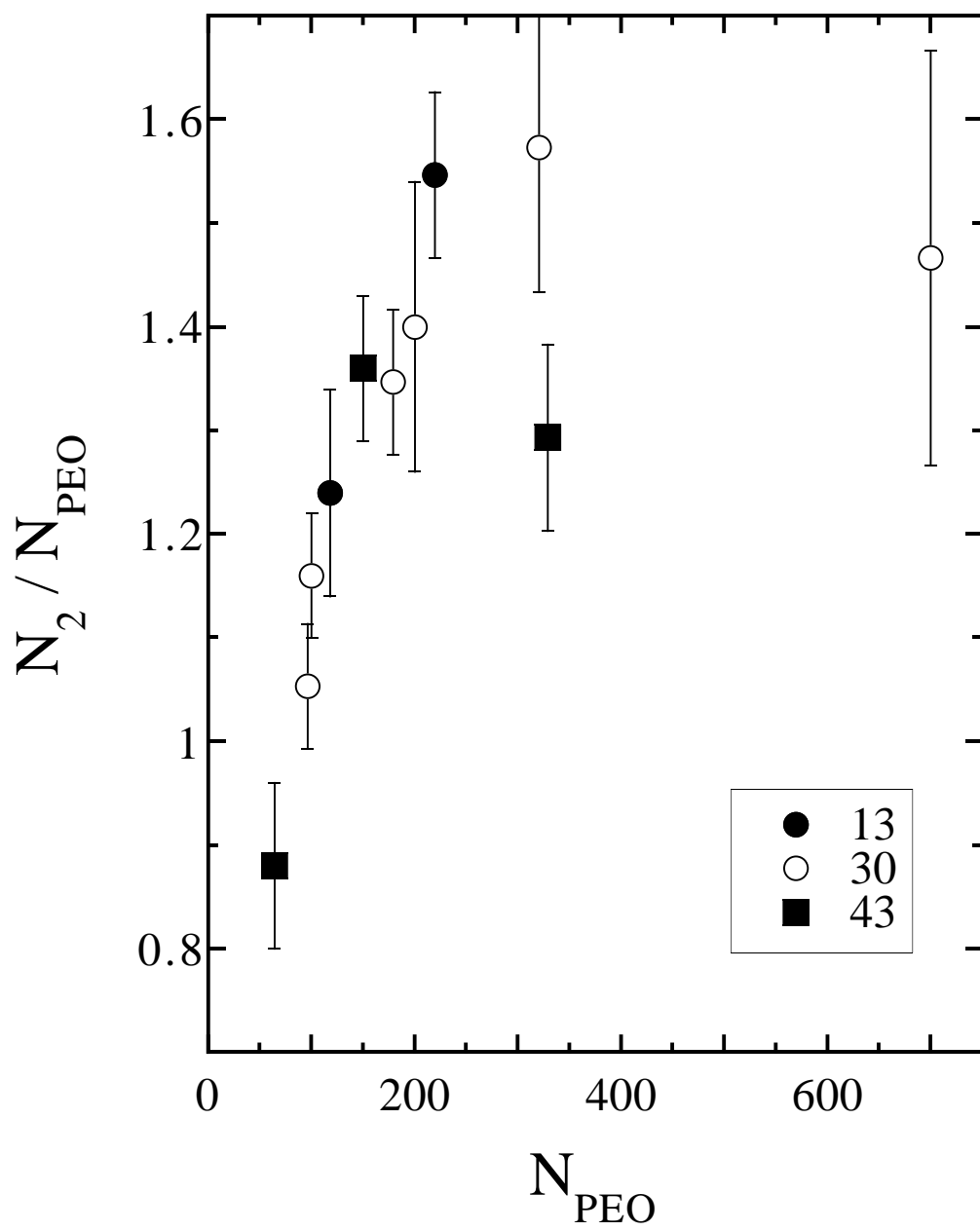


Fig. 8

N _{PS} -N _{PEO}	M _w (g/mole)	Polydispersity
0-205	9000	1.10
13-118	6 500	1.10
13-220	11 000	1.14
30-100	7 300	1.10
30-200	11 400	1.12
31-96 (D)	7 500	1.10
31-179 (D)	11 500	1.13
31-320 (D)	17 500	1.14
31-700 (D)	34 500	1.18
43-64	7 300	1.09
43-150	11 080	1.11
43-329	19 000	1.13